Juvenile hormone and 20-hydroxyecdysone coordinately control the developmental timing of matrix metalloproteinase–induced fat body cell dissociation

Qiangqiang Jia[‡], Suning Liu[‡], Di Wen[§], Yongxu Cheng[¶], William G. Bendena[||], Jian Wang[**1], and Sheng Li[2]

From the [‡]Guangzhou Key Laboratory of Insect Development Regulation and Application Research, Institute of Insect Science and Technology & School of Life Sciences, South China Normal University, Guangzhou 510631, China, the [§]Department of Life Science, Qiannan Normal College for Nationalities, Duyun, Guizhou 558000, China, the [¶]College of Fisheries and Life Science, Shanghai Ocean University, Shanghai 201306, China, the [||]Department of Biology, Queen's University, Kingston, Ontario K7L 3N6, Canada, and the [**]Department of Entomology, University of Maryland, College Park, Maryland 20742

Edited by Ronald C. Wek

Tissue remodeling is a crucial process in animal development and disease progression. Coordinately controlled by the two main insect hormones, juvenile hormone (JH) and 20-hydroxyecdysone (20E), tissues are remodeled context-specifically during insect metamorphosis. We previously discovered that two matrix metalloproteinases (Mmps) cooperatively induce fat body cell dissociation in *Drosophila*. However, the molecular events involved in this Mmp-mediated dissociation are unclear. Here we report that JH and 20E coordinately and precisely control the developmental timing of Mmp–induced fat body cell dissociation. We found that during the larval–prepupal transition, the anti-metamorphic factor Kr-h1 transduces JH signaling, which directly inhibited *Mmp* expression and activated expression of tissue inhibitor of metalloproteinases (*timp*) and thereby suppressed Mmp–induced fat body cell dissociation. We also noted that upon a decline in the JH titer, a prepupal peak of 20E suppresses Mmp–induced fat body cell dissociation through the 20E primary-response genes, *E75* and *Blimp-1*, which inhibited expression of the nuclear receptor and competence factor *βftz-F1*. Moreover, upon a decline in the 20E titer, *βftz-F1* expression was induced by the 20E early–late response gene *DHR3*, and then βftz-F1 directly activated *Mmp* expression and inhibited *timp* expression, causing Mmp–induced fat body cell dissociation during 6–12 h after puparium formation. In conclusion, coordinated signaling via JH and 20E finely tunes the developmental timing of Mmp–induced fat body cell dissociation. Our findings shed critical light on hormonal regulation of insect metamorphosis.

Tissue remodeling plays crucial roles during animal development and disease progression. The fat body in the fruit fly, *Drosophila melanogaster*, which is analogous to the vertebrate liver and adipose tissue, has emerged as an excellent model to study tissue remodeling (1, 2). The larval fat body is a single-cell layer and consists of only one cell type. During the prepupal–pupal transition, the larval fat body begins to lose its polygonal shape and becomes spherical, ~6 h after puparium formation (APF)[3] and completely dissociates into single and unattached cells during pupation (~12 h APF) (1–3). Notably, both matrix metalloproteinases (Mmp1 and Mmp2) are required to induce fat body cell dissociation in *Drosophila* (2, 3). We previously showed that Mmp1 preferentially cleaves *Drosphila* epithelial-cadherin–mediated cell–cell junctions, whereas Mmp2 preferentially degrades basement membrane (BM) components and thus destroys cell–BM junctions, resulting in the complete dissociation of fat body tissues into individual cells (2).

MMPs are extracellular Zn^{2+}-dependent endopeptidases that are responsible for degrading cell–cell junctions, cell–BM junctions, and BM components. *In vivo*, Mmp activities are finely tuned at different levels, from gene expression to zymogen activation and endogenous inhibition. In terms of endogenous inhibition, Mmps are typically regulated by TIMP (tissue inhibitor of metalloproteinases) (4). Although vertebrates contain more than 20 Mmps and 4 TIMPs, *Drosophila* possesses only two *Mmp*s and a single *timp* (5, 6). In addition, although Mmps induce fat body cell dissociation, *timp* overexpression suppresses fat body cell dissociation in *Drosophila* (2).

Developmental transitions in *Drosophila* are regulated by two major insect hormones: the steroid 20-hydroxyecdysone (20E) and the sesquiterpenoid juvenile hormone (JH). Two pulses of 20E, in conjunction with the nuclear receptor complex consisting of the ecdysone receptor (EcR) and ultraspiracle, were shown to induce larval–prepupal–pupal metamorphosis (7). Specifically, during the larval–prepupal transition, 20E induces the expression of several 20E primary-response genes, including *E74* (*Ecdysone-induced protein 74*), *E75*, *E93*, *Br-C* (*Broad complex*), and *Blimp-1* (*B lymphocyte-induced maturation protein 1*) (8). The 20E early–late response gene *DHR3*

[3] The abbreviations used are: APF, after puparium formation; 20E, 20-hydroxyecdysone; JH, juvenile hormone; Mmp, matrix metalloproteinase; TIMP, tissue inhibitor of matrix metalloproteinase; BM, basement membrane; EcR, ecdysone receptor; Met, methoprene-tolerant; JHRR, JH response region; KBS, Kr-h1–binding sites; qPCR, quantitative real-time PCR; IW, initiation of wandering; AIW, after IW; WPP, white prepupal stage; FBS, βftz-F1-binding site.

controls the termination of the 20E signal pulse during the larval–prepupal transition; DHR3 also induces the expression of *βftz-F1*, which acts as a competence factor for EcR-ultraspiracle to respond to the subsequent 20E signal pulse during the prepupal–pupal transition. Importantly, E75 prevents DHR3-mediated inhibition of 20E signaling and DHR3-induced *βftz-F1* expression through physical interaction and competition for retinoic acid receptor–related response elements (9–13). Moreover, Blimp-1 acts as a transcriptional repressor to restrict *βftz-F1* expression (14). Therefore, the 20E-induced transcriptional cascade, including E75, Blimp-1, DHR3, and βftz-F1, governs the two 20E signal pulses during *Drosophila* metamorphosis (8, 14). The two 20E pulses are likely involved in the regulation of fat body cell dissociation in *Drosophila*: blockade of the 20E receptor prevents fat body cell dissociation (15), whereas *βftz-F1* overexpression induces *Mmp2* expression and premature fat body cell dissociation (3). However, detailed studies are required to clarify the precise molecular mechanisms by which the two 20E pulses regulate fat body cell dissociation.

JH prevents 20E-induced metamorphosis via the JH receptor methoprene-tolerant (Met, a bHLH-PAS transcription factor) and the JH primary-response gene *Kr-h1* (Krüppel homolog 1, encoding a zinc finger transcription factor) (16, 17). There are two JH receptors in *Drosophila*: Met and its paralog gce (germ-cell expressed) (18–21). In the presence of JH, Met/gce binds to a JH response region (JHRR) in the *Kr-h1* promoter and directly induces *Kr-h1* expression (22–24). Notably, Kr-h1 directly represses the expression of two crucial 20E primary-response genes: *Br-C* and *E93* (22, 25, 26). Moreover, Kr-h1–binding sites (KBSs) were identified in the promoter regions of *Br-C* and *E93* in the silkworm, *Bombyx mori*, with a consensus sequence TGACCTNNNNYAAC (27, 28). Kr-h1–mediated inhibition of the expression of 20E response genes at least partially accounts for the cross-talk between JH and 20E; thus, Kr-h1 is considered as an anti-metamorphic factor in insects (16, 17). Interestingly, we observed precocious fat body cell dissociation in both JH-deficient animals and *Met gce* double mutant animals (19, 29). However, nothing is known about whether and how Kr-h1 mediates JH signals to inhibit fat body cell dissociation in *Drosophila*.

During insect metamorphosis, a series of cellular events, including programmed cell death, cell proliferation, cell differentiation, and cell dissociation, occurs in a context-specific manner. Previous investigations indicate all of the events are coordinately controlled by JH and 20E (7, 16, 17, 27). However, our current understanding of how the same two hormones induce different cellular processes at distinct, yet precise, developmental timing is very limited. Here, we discovered that JH and 20E coordinately and precisely control the developmental timing of Mmp–induced fat body cell dissociation in *Drosophila* at both the mRNA and enzymatic levels. This study provides an example to better understand hormonal regulation of tissue remodeling during insect metamorphosis.

Results

Kr-h1 transduces JH signaling to repress Mmp expression

The developmental timing of fat body cell dissociation is strictly controlled in *Drosophila* and occurs only within a small window immediately before pupation, from 6 h APF to 12 h APF (1, 2). Consistent with our previous reports (19, 29), enhanced fat body cell dissociation was observed in both JH-deficient animals (*Aug21-Gal4>UAS-grim*) and *Met gce* double mutant (*Met^27gce^2.5k*) at 6 h APF compared with wild-type animals (*w^1118*) (Fig. 1*A* and Fig. S1). Likewise, the *Kr-h1* mutant (*Kr-h1^k04411*) showed enhanced fat body cell dissociation at 6 h APF. By contrast, fat body cell dissociation was inhibited at 12 h APF when *Kr-h1* was specifically overexpressed in the fat body (*Lsp2-Gal4>UAS-Kr-h1*) (Fig. 1*A* and Fig. S1).

According to our previous study, Mmp1 and Mmp2 cooperatively induce *Drosophila* fat body cell dissociation, each assuming a distinct role (2). Therefore, we examined whether JH signaling prevents fat body cell dissociation by regulating *Mmp* expression. We performed a Western blot analysis (2), and detected increased protein levels for both Mmps at 6 h APF in the fat body of animals lacking JH signaling, including *Aug21-Gal4 > UAS-grim*, *Met^27gce^2.5k*, and *Kr-h1^k04411*, whereas protein levels decreased at 12 h APF in the fat body of the *Kr-h1*–overexpressing animals, *Lsp2-GAL4 > UAS-Kr-h1* (Fig. 1*B*). Using quantitative real-time PCR (qPCR), we also detected up-regulated mRNA levels for both *Mmp*s at 6 h APF in the fat body of animals lacking JH signaling and down-regulated mRNA levels at 12 h APF in the fat body of the *Kr-h1*–overexpressing animals (Fig. 1, *C* and *D*).

After examining the role of Kr-h1 in regulating *Mmp* expression and fat body cell dissociation, we determined its developmental profile in the fat body. We previously reported that the JHRR-*LacZ* reporter recapitulates the responsiveness of *Kr-h1* to JH and Met/gce (24). Immunohistochemistry indicated that JHRR-LacZ was non-detectable in the fat body of the feeding larvae, emerged upon the initiation of wandering (IW), peaked at 3 h after IW (AIW), gradually decreased from 6 h AIW to the white prepupal stage (WPP), and became barely detectable at 3 h APF (Fig. 1*E*). These results were consistent with previous reports describing developmental profiles for JH titers (21, 30). Interestingly, we found that the developmental profile of *Kr-h1* expression was several hours delayed when compared with that of JHRR-LacZ. *Kr-h1* mRNA levels in the fat body of *w^1118* animals gradually increased upon IW to 3 h APF but dramatically decreased thereafter (Fig. 1*F*). The developmental profile for *Kr-h1* mRNA expression corroborates previous findings (22, 31), indicating that it should be activated by both JH and 20E with overlapping effects. The detailed molecular mechanisms by which JH and 20E coordinately induce *Kr-h1* expression warrant further investigation. Nevertheless, the experimental data show that the anti-metamorphic factor Kr-h1 transduces JH signaling to repress *Mmp* expression and prevent fat body cell dissociation during the larval–prepupal transition in *Drosophila*.

Identification of KBS in Mmp1 promoter

We next examined whether *Kr-h1* overexpression in *Drosophila* Kc cells represses *Mmp* expression to the same extent as that in the fat body. Although *Mmp2* expression was not significantly repressed, the down-regulation of *Mmp1* expression was significant (Fig. 2*A*). Thus, we focused on investigating how Kr-h1 represses *Mmp1* expression in Kc cells.
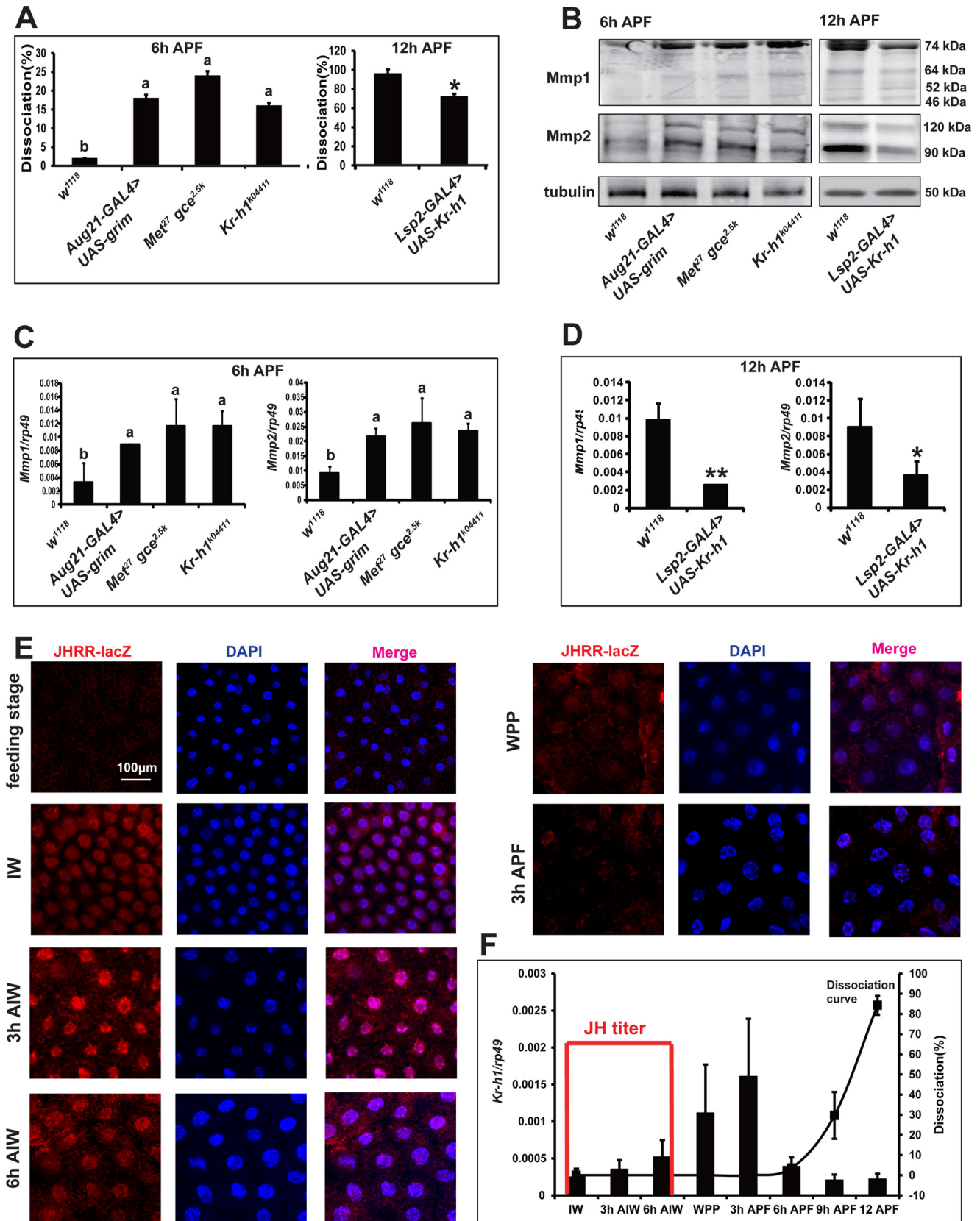
Figure 1. Kr-h1 transduces JH signaling to repress *Mmp* expression. *A*, compared with w^{1118} animals, fat body cell dissociation in JH signaling-deficient animals at 6 h APF (*left*) and *Kr-h1*– overexpressing animals at 12 h APF (*right*). *B*, compared with w^{1118} animals, Mmps protein levels in the fat body of JH signaling-deficient animals at 6 h APF (*left*) and in the fat body of *Kr-h1*– overexpressing animals at 12 h APF (*right*). *C* and *D*, compared with w^{1118} animals, *Mmps* mRNA levels in the fat body of JH signaling-deficient animals at 6 h APF (*C*) and in the fat body of *Kr-h1*– overexpressing animals at 12 h APF (*D*). *E* and *F*, developmental profiles of JHRR-LacZ (*E*), JH levels, *Kr-h1* mRNA levels in fat body, and fat body cell dissociation (*F*) of w^{1118} animals at 3-h intervals. In *F*, the JH titer is depicted according to Dubrovsky 2005 (30); the *columns* show mRNA level of *Kr-h1*, and the *curve* shows the degree of fat body dissociation.
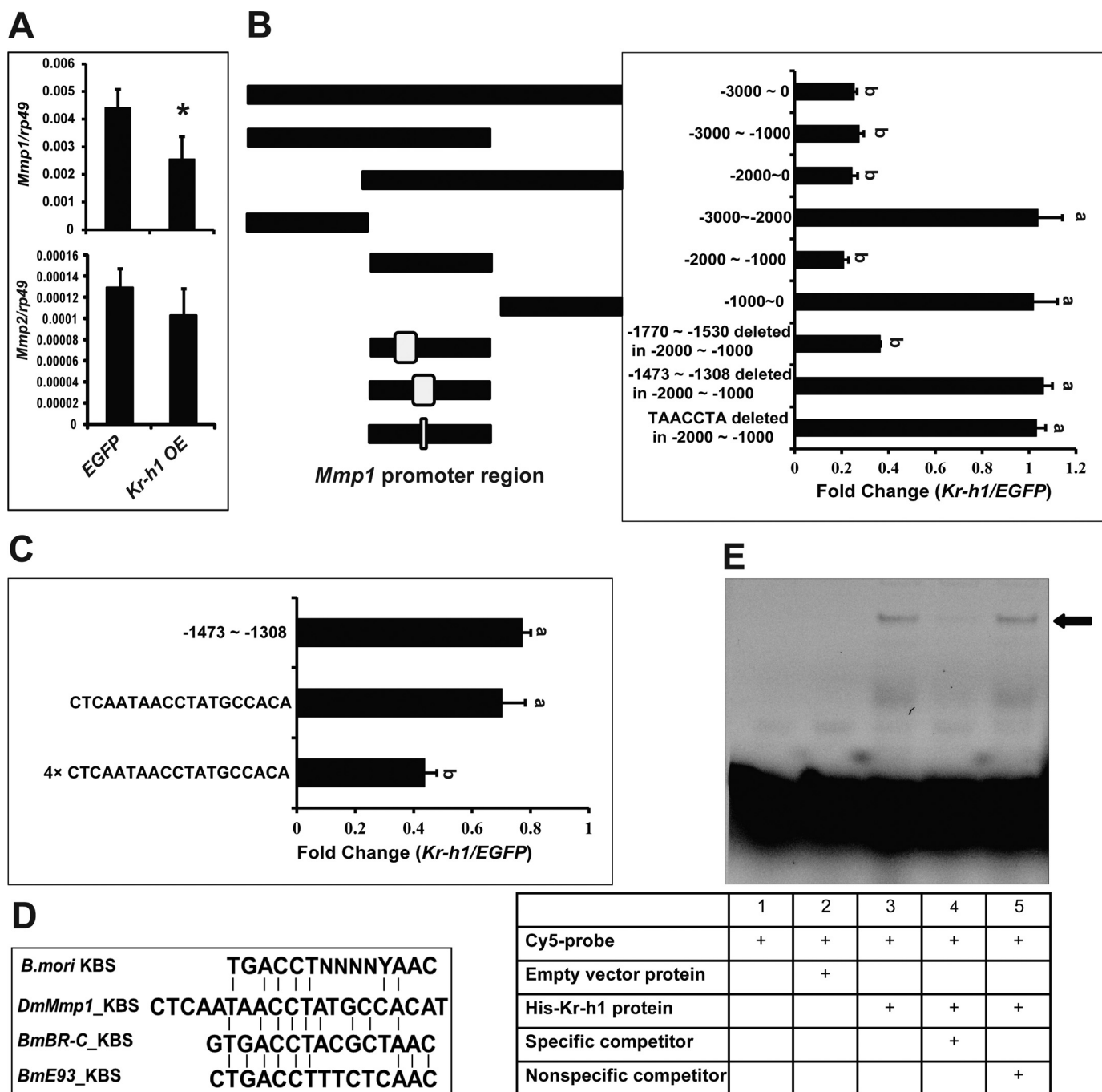
Figure 2. Identification of a KBS in *Mmp1* promoter. *A*, *Mmp*s mRNA levels in *EGFP*-overexpressing (as a control) and *Kr-h1*– overexpressing *Drosophila* Kc cells. *B* and *C*, dual luciferase assay. Kc cells were co-transfected with a *Kr-h1* expression construct (*EGFP* was used as a control) and pGL3-basic plasmids containing different lengths of the *Mmp1* promoter region or the −2000 to −1000 fragment with specific deletions (*B*). From the localization in *B*, a sequence was identified in a fragment −1473 to −1308 and a specific sequence CTCAATAACCTATGCCACAT (KBS) in one or four copies (*C*). Dual luciferase assays were performed at 48 h post-transfection. The luciferase activity fold change was defined as the relative luciferase activity induced by *Kr-h1* overexpression compared with *EGFP* overexpression. *D*, alignment of KBS in promoters of silkworm *Br-C* and *E93* and *Drosophila Mmp1*. *E*, EMSA. His-Kr-h1 protein was purified from *E. coli* and incubated with a three times repeated KBS probe labeled with Cy5 for 2 h. Competition assays were performed using 100-fold molar excess of unlabeled specific or nonspecific probes.

To identify the Kr-h1 response region in the *Mmp1* promoter, we employed a dual luciferase assay system and Kc cells. A 3-kb promoter region of *Mmp1* (−3000 to 0 upstream of the transcriptional start site) was cloned into the pGL3-Basic vector. Upon *Kr-h1* overexpression, this promoter region exhibited ∼25% of the luciferase activity achieved with *EGFP* overexpression (Fig. 2*B*). Five truncated regions were also cloned

into the pGL3-Basic vector, and *Kr-h1* overexpression inhibited three truncated regions (−3000 to −1000, −2000 to 0, and −2000 to −1000) the same degree as the 3-kb promoter region (Fig. 2*B*). Considering some preliminary ChIP and qPCR results, we deleted two small fragments (−1770 to −1530 and −1473 to −1308) from the −2000 to −1000 region in the pGL3-Basic vector. Although the former construct still exhib-

ited similar inhibitory responses, the latter showed no response to *Kr-h1* overexpression (Fig. 2*B*). The −1473 to −1308 fragment was then cloned into the pGL3-promoter vector, which responded to *Kr-h1* inhibition (Fig. 2*C*).

KBSs were previously identified in the promoter regions of *Br-C* and *E93* in the silkworm (27, 28), and we searched to determine whether the consensus sequence TGACCTNNNNYAAC was also conserved in the −1473 to −1308 region of the *Drosophila Mmp1* promoter. We found a sequence, CTCAATAACCTATGCCACAT (−1407 to −1427), that was similar to the consensus sequence above (Fig. 2*D*). After the core consensus sequence TAACCTA was deleted from the −2000 to −1000 fragment-containing pGL3-Basic vector, the promoter region did not respond to *Kr-h1* inhibition any longer (Fig. 2*B*). Then either one copy or four copies of CTCAATAACCTATGCCACAT were individually cloned into the pGL3-promoter vector. One copy of the sequence produced an inhibitory response similar to the −1473 to −1308 fragment, whereas four copies of the sequence resulted in luciferase activity that was reduced by half compared with that with *EGFP* overexpression (Fig. 2*C*), suggesting the sequence CTCAATAACCTATGCCACAT in the *Mmp1* promoter is a KBS.

To validate this hypothesis, we performed EMSA with three tandem repeats of CTCAATAACCTATGCCACAT and His tag–purified Kr-h1 protein. Importantly, Kr-h1 and CTCAATAACCTATGCCACAT formed a protein–DNA complex. In competition assays, the specific band disappeared upon the addition of 100-fold molar excess of an unlabeled probe but not a nonspecific competitor (Fig. 2*E*). Thus, our experimental data identified a true KBS in the *Mmp1* promoter. In conclusion, Kr-h1 transduces JH signaling to repress fat body cell dissociation through the direct inhibition of *Mmp1* expression during the larval–prepupal transition.

EcR and βftz-F1 are required for Mmp expression

To better understand how the two 20E pulses regulate fat body cell dissociation during *Drosophila* metamorphosis, we first re-examined the roles of EcR and βftz-F1 in this process (3, 15). When a dominant-negative mutant of *EcR* (*EcR^DN^*) was overexpressed (*Lsp2-Gal4>UAS-EcR^DN^*) or βftz-F1 expression was reduced by RNAi (*Lsp2-Gal4>UAS-βftz-F1-dsRNA*), fat body cell dissociation was inhibited at 12 h APF. By contrast, when βftz-F1 was overexpressed (*Lsp2-Gal4>UAS-βftz-F1*), fat body cell dissociation increased 10-fold at 6 h APF (Fig. 3*A* and Fig. S2). According to the results of Western blotting analyses, protein levels of both Mmps decreased in *EcR^DN^*-overexpressing and βftz-F1-RNAi fat body and increased in βftz-F1-overexpressing fat body (Fig. 3*B*). The results of qPCR analysis revealed that mRNA levels of both *Mmps* were similarly regulated by *EcR* and βftz-F1 (Fig. 3, *C* and *D*). It is of note that the regulatory effect of EcR and βftz-F1 on Mmp2 is much stronger than Mmp1 (Fig. 3, *B–D*). Significantly, βftz-F1 mRNA levels in the fat body were comparatively low from IW to 3 h APF, sharply increased until 9h APF, and decreased at 12 h APF (Fig. 3*E*), indicating that the developmental profile of βftz-F1 mRNA is similar to but slightly ahead of that for fat body cell dissociation. Finally, we determined whether βftz-F1 overexpression in Kc cells increased *Mmp* expression to the same extent

as that in the fat body. Again, expression of both *Mmps* was up-regulated, but the up-regulation of *Mmp2* expression was much more significant (Fig. 3*F*). We next investigated whether E75, DHR3, and Blimp-1 convert signals of the first 20E pulse to βftz-F1 at the second 20E pulse to induce *Mmp* expression and thus Mmp–induced fat body cell dissociation before pupation.

E75, DHR3, and Blimp-1 elaborately regulate expression of βftz-F1 and Mmps

Previous reports indicate the 20E primary-response gene *E75* prevents DHR3 transactivation of βftz-F1 expression (9–13). Therefore, we verified whether the 20E-triggered transcriptional cascade, involving *E75*, *DHR3*, and βftz-F1, was conserved in the regulation of fat body cell dissociation. Although fat body dissociation visually appeared to be reduced upon *E75A* overexpression or *DHR3* depletion alone (Fig. S3), only the combination of both treatments inhibited the tissue dissociation significantly when quantified (Fig. 4*A*). By contrast, depletion of *E75* or overexpression of *DHR3* in the fat body led to increased tissue dissociation at 6 h APF, and combined manipulation of both genes had an additive effect (Fig. 4*A* and Fig. S3).

We then investigated the role of E75 and DHR3 in regulating the expression of *E75*, *DHR3*, βftz-F1, and *Mmp*s in the fat body. At 12 h APF, *E75A* overexpression had no effect on *DHR3* expression but significantly repressed the expression of βftz-F1 and *Mmp*s; *DHR3* RNAi had no effect on *E75* expression but significantly repressed the expression of βftz-F1 and *Mmp*s; and simultaneous *E75A* overexpression and *DHR3* RNAi exerted additive effects (Fig. 4*B*). By contrast, at 6 h APF, *E75* RNAi had no effect on *DHR3* expression but significantly induced the expression of βftz-F1 and *Mmp*s, *DHR3* overexpression had no effect on *E75* expression but significantly induced the expression of βftz-F1 and *Mmp*s, and simultaneous *E75* RNAi and *DHR3* overexpression exerted additive effects (Fig. 4*C*).

The 20E primary-response gene *Blimp-1* acts as a transcriptional repressor for βftz-F1 (14). When *Blimp-1* expression was inhibited by RNAi (*Lsp2-Gal4>UAS-Blimp-1-dsRNA*) or *Blimp-1* was overexpressed (*Lsp2-Gal4>UAS-Blimp-1*), fat body cell dissociation was inhibited at 12 h APF and increased at 6 h APF, respectively (Fig. 4*A* and Fig. S4). *Blimp-1* RNAi increased the expression of βftz-F1 and *Mmp*s, whereas *Blimp-1* overexpression had the opposite effect. In addition, *Blimp-1* overexpression in Kc cells repressed the expression of βftz-F1 and *Mmp*s (Fig. 4*D*).

To gain additional insights into the regulation of fat body cell dissociation by *E75*, *DHR3*, and *Blimp-1*, we determined developmental profiles of mRNA expression in the fat body at 3-h intervals. Expression of *E75*, *Blimp-1*, and *DHR3* peaked at 6 h AIW, WPP, and 3 h APF, respectively (Fig. 4*E*). Thus, we assume that E75 represses DHR3 transactivation of βftz-F1 expression, and Blimp-1 directly represses βftz-F1 expression during the larval–prepupal transition; moreover, DHR3 directly induces βftz-F1 expression during the prepupal–pupal transition.
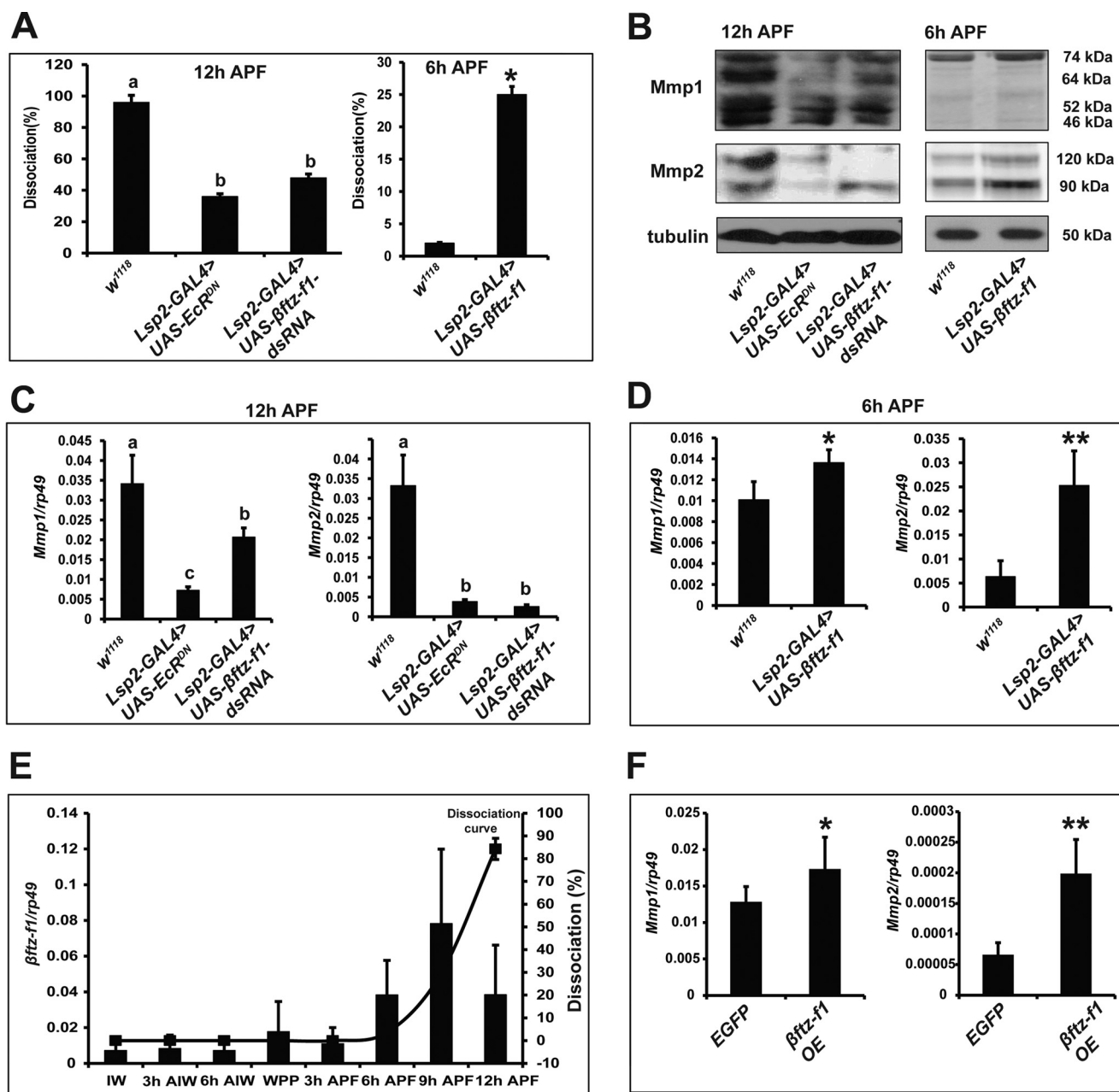
Figure 3. EcR and βftz-F1 are required for *Mmp* expression. *A*, fat body cell dissociation in *EcR^DN*-overexpressing and *βftz-F1* down-regulated animals at 12 h APF (*left panel*) and *βftz-F1*-overexpressing animals at 6 h APF (*right panel*). *B*, *Mmp*s protein levels in the fat body of *EcR^DN*-overexpressing and *βftz-F1* RNAi animals at 12 h APF (*left panel*) and in the fat body of *βftz-F1*-overexpressing animals at 6 h APF (*right panel*). *C* and *D*, *Mmp*s mRNA levels in the fat body of *EcR^DN*-overexpressing and *βftz-F1* down-regulated animals at 12 h APF (*C*) and in the fat body of *βftz-F1*-overexpressing animals at 6 h APF (*D*). *E*, the *columns* show developmental changes in the mRNA levels of *βftz-F1* in fat body, and the *curve* shows the degree of fat body dissociation of *w^1118* animals at 3-h intervals. *βftz-F1* mRNA levels peak at 9 h APF. *F*, *Mmp*s mRNA levels in *EGFP*-overexpressing (as a control) and *βftz-F1*-overexpressing Kc cells.

Identification of a F1-binding site (FBS) in Mmp2 promoter

To this end, we examined whether βftz-F1 induces *Mmp2* expression directly or indirectly using the dual luciferase assay system and Kc cells. A 3-kb *Mmp2* promoter region was cloned into the pGL3-Basic vector. Upon βftz-F1 overexpression, this promoter region supported an ∼4-fold increase in luciferase activity (Fig. 5*A*). Five truncated regions (−3000 to −1000, −2000 to 0, −3000 to −2000, −2000 to −1000, and −1000 to 0) were cloned into the pGL3-Basic vector. Based on the results of dual luciferase assay, βftz-F1 response elements exist in a distal region of the *Mmp2* promoter (−3000 to −2000) (Fig. 5*A*).

Previous studies suggest the monomeric FBS consensus sequence is PyCAAGGPyCPu or PyGAAGGPyCPu (36). Three possible FBSs were predicted in the 3-kb promoter region of *Mmp2*: GGAAGGTCA (−2604 to −2595), AGGCCTTGA (−2326 to −2317), and TCAAGGCTG (−1254 to −1263) (Fig. 5*B*). After *FLAG-βftz-F1* was overexpressed in Kc cells, ChIP-qPCR was performed to examine whether βftz-F1 directly binds to these potential FBSs to induce *Mmp2* expression. As measured by qPCR, a FLAG antibody increased the precipitation of the first possible FBS but not the other two (Fig. 5*C*).
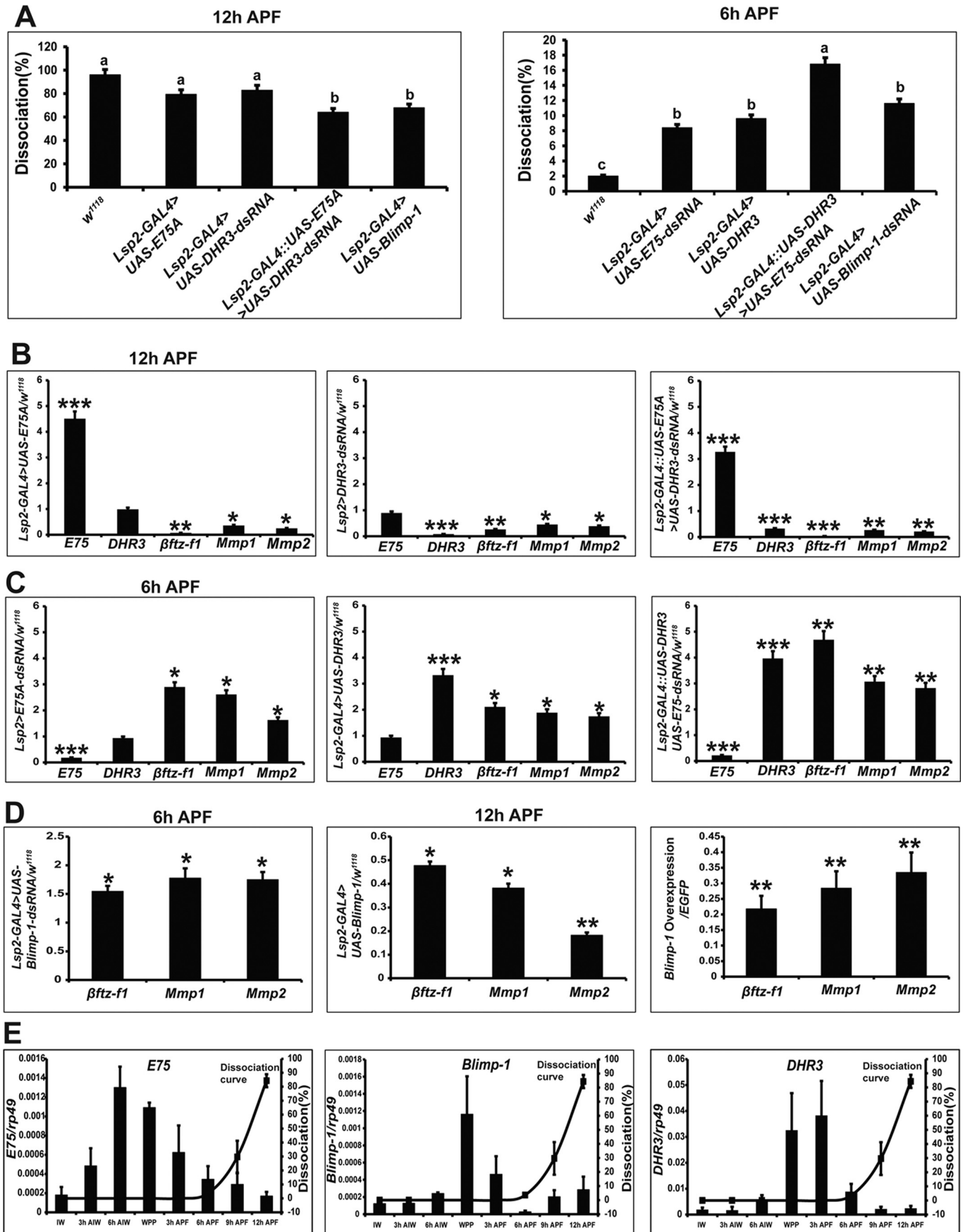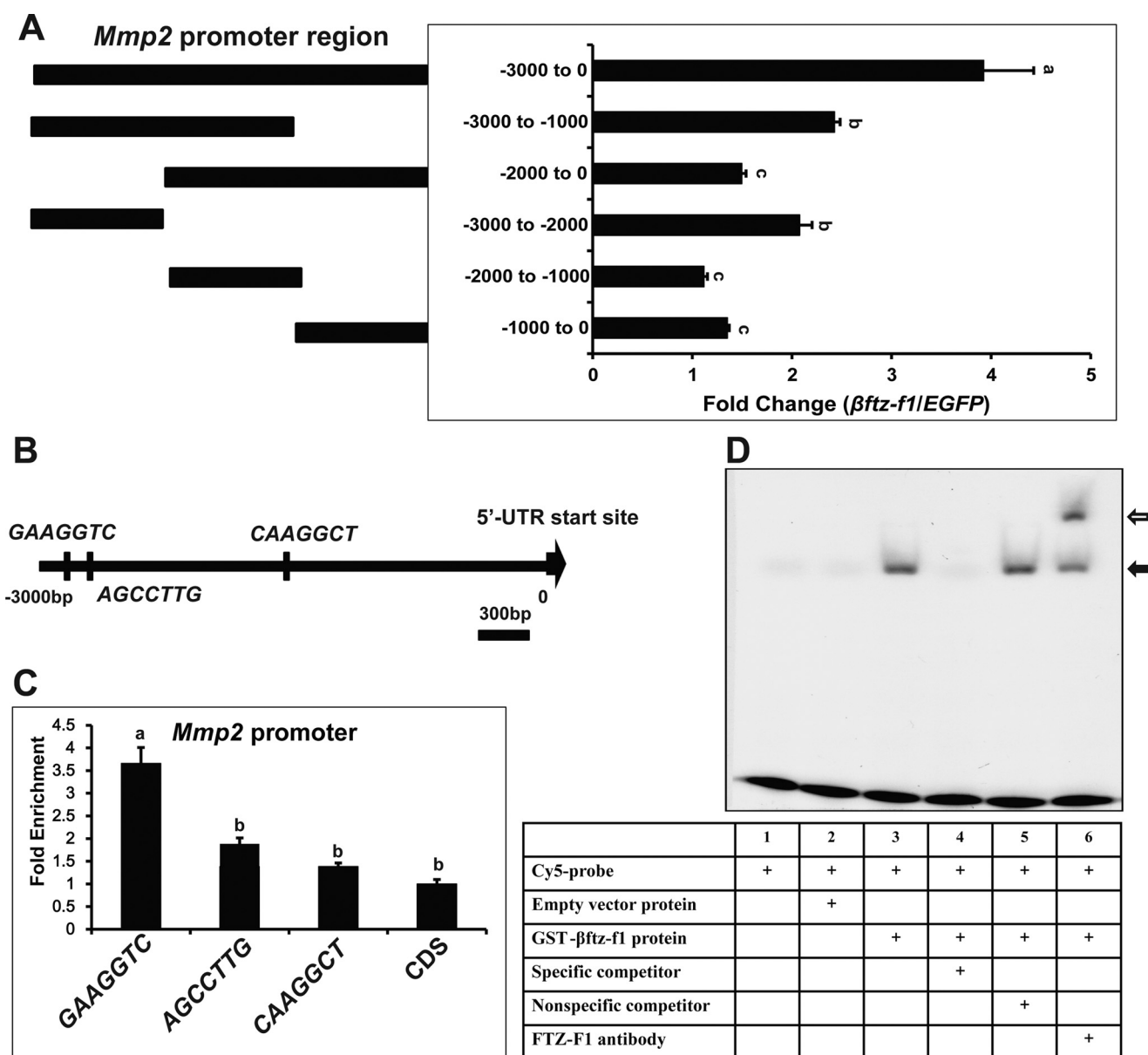
Figure 5. Identification of a FBS in *Mmp2* promoter. *A*, dual luciferase assay. Kc cells were co-transfected with a *βftz-F1* expression construct (EGFP was used as a control), along with pGL3-basic plasmids containing *Mmp2* promoter regions of different lengths. After 48 h of transfection, dual luciferase assays were performed. The luciferase activity fold change is defined as the relative luciferase activity induced by *βftz-F1* overexpression compared with EGFP overexpression. *B*, locations of three *βftz-F1* putative binding sites within the *Mmp2* 3-kb promoter. *C*, ChIP-qPCR. At 48 h after transfection, *FLAG-βftz-F1*-overexpressing Kc cells were fixed and subjected to ChIP using a FLAG mouse monoclonal antibody. Mock immunoprecipitations with preimmune serum were performed as negative controls. The precipitated DNA (different fragments in the 3-kb promoter region of *Mmp2*) and input were analyzed by qPCR to detect binding ability. *D*, EMSA. We used a three times repeated TGGGGGAAGGTCAAAT sequence (KBS), corresponding to a site located in the −2604 to −2595 region upstream of the *Mmp2* transcription start site. A Cy5-labeled *βftz-F1* binding site was added to a mixture with GST-*βftz-F1* fusion proteins, in the presence (*lane 4*) or absence (*lane 5*) of an unmodified competitor. A supershift band was observed when a FTZ-F1 antibody was added into the reaction mixture.

To verify that this sequence was a genuine FBS, we examined whether three tandem repeats of TGGGGGAAGGTCAAAT (−2607 to −2592) bound to GST-purified *βftz-F1* protein in an EMSA experiment (Fig. 5*D*). *βftz-F1* and TGGGGGAAGGTCAAAT formed a protein–DNA complex with a specific band shift that was supershifted by the addition of a *βftz-F1* antibody.

Figure 4. E75, DHR3, and Blimp-1 regulate the expression of *Mmps* and *βftz-F1*. *A*, fat body cell dissociation in animals in which *E75A* was overexpressed, *DHR3* expression was reduced by RNAi, combined *E75A* overexpression and *DHR3* RNAi, and *Blimp* was overexpressed at 12 h APF (*left panel*). Fat body cell dissociation in animals in which *DHR3* was overexpressed, *E75* expression was reduced by RNAi, combined *DHR3* overexpression and *E75* RNAi, and *Blimp* expression was reduced by RNAi at 6 h APF (*right panel*). *B*, *βftz-F1* and *Mmp* expression in the fat body of *E75A* overexpression (*left panel*), *DHR3* RNAi (*middle panel*), and combined *E75A* overexpression and *DHR3* RNAi (*right panel*) animals. *C*, *βftz-F1* and *Mmp* expression in the fat body of *E75* RNAi (*left panel*), *DHR3* overexpression (*middle panel*), and combined *E75*-RNAi and *DHR3* overexpression animals (*right panel*). *D*, *βftz-F1* and *Mmp* expression levels in the *Blimp-1* RNAi fat body (*left panel*); *βftz-F1* and *Mmp* expression levels in the *Blimp-1* overexpressing fat body (*middle panel*) and Kc cells (*right panel*). *E*, the *columns* show developmental changes in mRNA levels of *E75* (*left panel*), *Blimp-1* (*middle panel*), and *DHR3* (*right panel*) in the fat body, and the *curve* shows the degree of fat body dissociation in w^{1118} animals at 3-h intervals.

Competition assays showed that the specific band disappeared upon the addition of 100-fold molar excess of an unlabeled probe but not a nonspecific competitor. Thus, a genuine FBS was identified from the *Mmp2* promoter.

Altogether, β*ftz-F1* expression is activated during the pre-pupal–pupal transition because of elaborate control exerted by the 20E-triggered transcriptional cascade, including *E75*, *Blimp-1*, and *DHR3*. When JH titer declines, the prepupal peak of 20E suppresses Mmp–induced fat body cell dissociation through the 20E primary-response genes, *E75* and *Blimp-1*, which inhibit β*ftz-F1* expression indirectly or directly. Until 20E titer declines, β*ftz-F1* expression is induced by the 20E early–late response gene *DHR3*; then β*ftz-F1* directly activates *Mmp* expression and causes Mmp–induced fat body cell dissociation occurring from 6 h APF to 12 h APF.

Kr-h1 activates and βftz-F1 inhibits timp expression

As mentioned in our previous reports (2), overexpression of *timp* in the fat body (*Lsp2-Gal4>UAS-timp*) completely blocks its cell dissociation, resulting in pupal lethality. By contrast, precocious fat body cell dissociation was observed in the *timp* mutant (*timp*[28]) (Fig. S5*B*). The above results agree with the notion that timp inhibits the enzymatic activity of Mmps in the fat body (2). Thus, we investigated whether and how JH- and 20E-mediated regulation of *timp* expression and thus the enzymatic activity of Mmps.

The mRNA levels of *timp* were down-regulated at 6 h APF in the fat body of animals lacking JH signaling and up-regulated at 12 h APF in the fat body of *Kr-h1*– overexpressing animals (Fig. 6*A*). By contrast, the mRNA levels of *timp* were up-regulated in *EcR*[DN]-overexpressing and *ftz-F1*-RNAi fat body at 12 h APF and down-regulated in β*ftz-F1*-overexpressing fat body at 6 h APF (Fig. 6*B*). The experimental data indicate that Kr-h1 transduces JH signaling to activate and β*ftz*-F1 mediates 20E signaling to inhibit *timp* expression, which could inhibit the enzymatic activity of Mmps and thus fat body cell dissociation.

Finally, we examined the enzymatic activity of Mmps in the above genotypes. Mmps activity significantly increased at 6 h APF in the fat body of the *timp* mutant, animals lacking JH signaling, and β*ftz*-F1-overexpressing animals and decreased at 12 h APF in the fat body of *timp*-overexpressing, *EcR*[DN]-over-expressing, β*ftz*-F1-RNAi, and *Kr-h1*– overexpressing animals (Fig. 6*C*). Thus, the enzymatic activity of Mmps for each genotype results from changes in the expression of both *Mmps* and *timp*. In summary, JH and 20E coordinately and precisely control Mmps activity at both mRNA and enzymatic levels so that fat body cell dissociation occurs within 6 h before pupation (Fig. 7).

Discussion

MMPs and TIMPs play crucial roles in regulating tissue remodeling in both vertebrates and *Drosophila* (4–6). Our previous work has demonstrated the collaborative functions of Mmp1 and Mmp2 in inducing fat body cell dissociation in *Drosophila* (2). *timp* mutant adults show autolyzed tissue in the abdominal cavity and inflated wings, a phenotype consistent with the role of timp in BM integrity and remodeling (33). The current study clarified the role of timp in inhibiting the enzy-

matic activity of Mmps and thus, Mmp–induced fat body cell dissociation (Fig. 6 and Fig. S4). In mammals, Mmps activity *in vivo* is controlled at different levels, including the regulation by gene expression, the zymogens activation, and the inhibition of active enzymes by TIMPs (33, 34). These studies unify the important inhibitory roles of timp/TIMP in regulating tissue remodeling in both *Drosophila* and mammals. In addition to regulating *Mmp* expression (Figs. 1–5), JH and 20E signals differentially regulate *timp* expression, with the stimulatory role of Kr-h1 and the inhibitory role of β*ftz*-F1 (Fig. 6). Because timp inhibits the enzymatic activity of Mmps in the *Drosophila* fat body (Fig. 6), we conclude that JH and 20E coordinately control Mmps activity at both the mRNA and enzymatic levels (Fig. 7).

We previously reported the requirement of both JH and its receptors to inhibit fat body cell dissociation in *Drosophila* (19, 29). Here, we demonstrated the ability of Kr-h1 to transduce JH signaling to decrease *Mmp* expression and to induce *timp* expression during larval–prepupal transition (Figs. 1 and 6). Moreover, a KBS was identified in the *Mmp1* promoter, indicating that Kr-h1 directly represses *Mmp1* expression (Fig. 2). Interestingly, *Kr-h1* expression gradually increases from IW to 3 h APF when induced by JH and 20E in an overlapping manner (Fig. 1*F*), thus inhibiting the enzymatic activity of Mmps and Mmp–induced fat body cell dissociation during the larval–prepupal transition. Moreover, Kr-h1 acts as an anti-metamorphic factor by inhibiting 20E signaling (16, 17). We propose, in addition to directly affecting the expression of *Mmp*s and *timp*, that Kr-h1 might also indirectly regulate their expression by inhibiting 20E signaling (Fig. 7).

Two consecutive 20E pulses control timely metamorphosis in *Drosophila* (8). Together with previous findings (3, 15), our results show that the conserved 20E transcriptional cascade precisely controls the timing of Mmp–induced fat body cell dissociation (Fig. 7). In general, the first 20E signal pulse plays an inhibitory role during the larval–prepupal transition; how-ever, it is a prerequisite for the expression of β*ftz-F1*, which induces the second 20E signal pulse during the prepupal–pupal transition and the expression of *Mmps*. Because of the require-ment for the first 20E signal pulse, blockade of the 20E receptor prevents fat body cell dissociation (Fig. 3). When JH titer declines, the prepupal peak of 20E activates expression of two 20E primary-response genes, *E75* and *Blimp-1*, to inhibit fat body cell dissociation: E75 represses DHR3 transactivation of β*ftz-F1* expression, and Blimp-1 directly represses β*ftz-F1* expression. During the prepupal–pupal transition, DHR3 directly induces β*ftz-F1* expression from 6 h APF to 12 APF (Fig. 4). Before pupation, β*ftz-F1* induces *Mmp* expression and represses *timp* expression (Figs. 3 and 6). Moreover, an FBS was identified in the *Mmp2* promoter, demonstrating that β*ftz*-F1 directly induces *Mmp2* expression (Fig. 5). Finally, within 6 h before pupation, Mmp1 and Mmp2 cooperatively induce fat body cell dissociation, with each assuming a distinct role (2).

Insect metamorphosis is coordinately controlled by JH and 20E, whereas the hormonal control of tissue remodeling is strictly context-specific. Different larval tissues and adult organs might have distinct, yet precise, developmental fates and timing (7, 8, 16, 17). Our knowledge regarding this question is poor. Based on previous preliminary information, we clarified
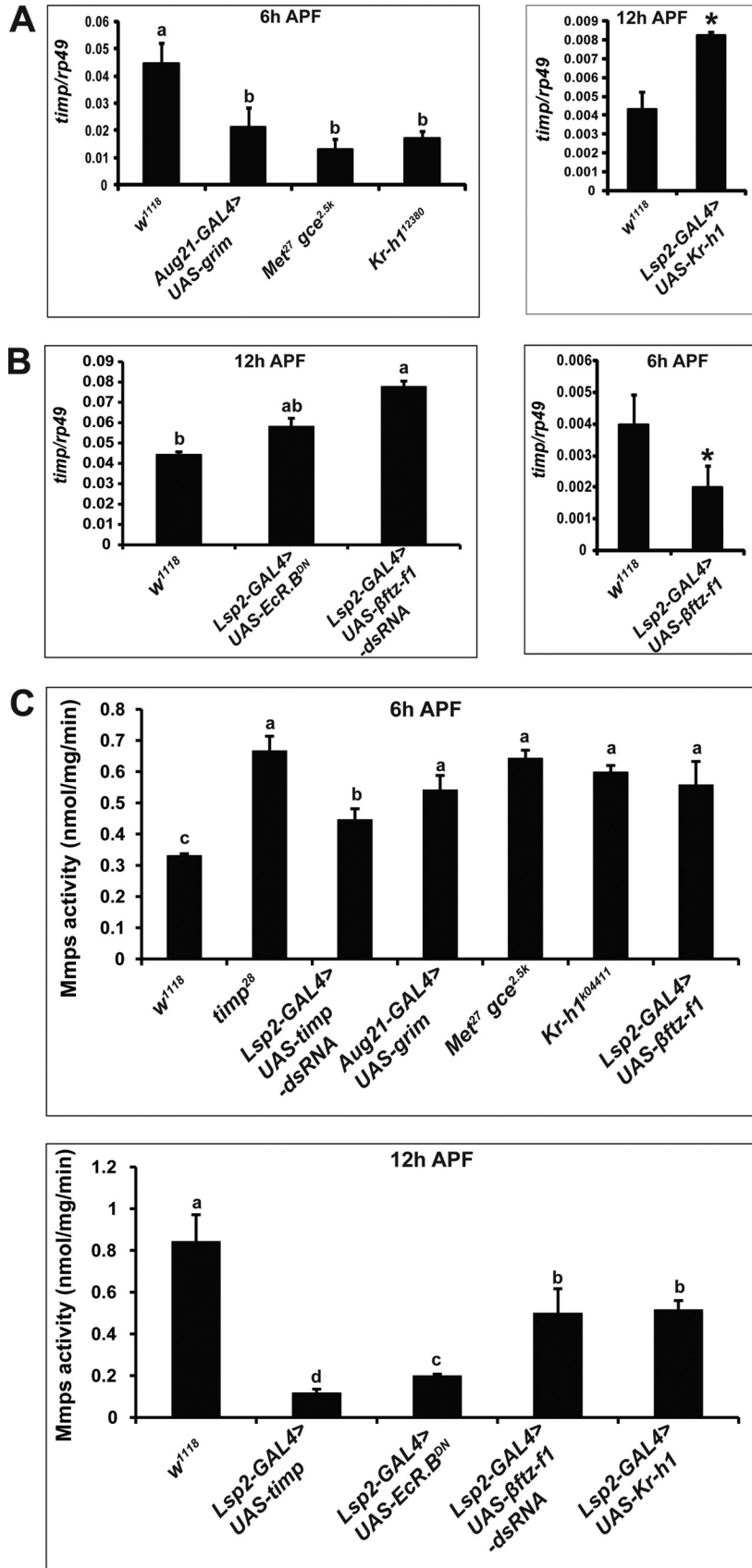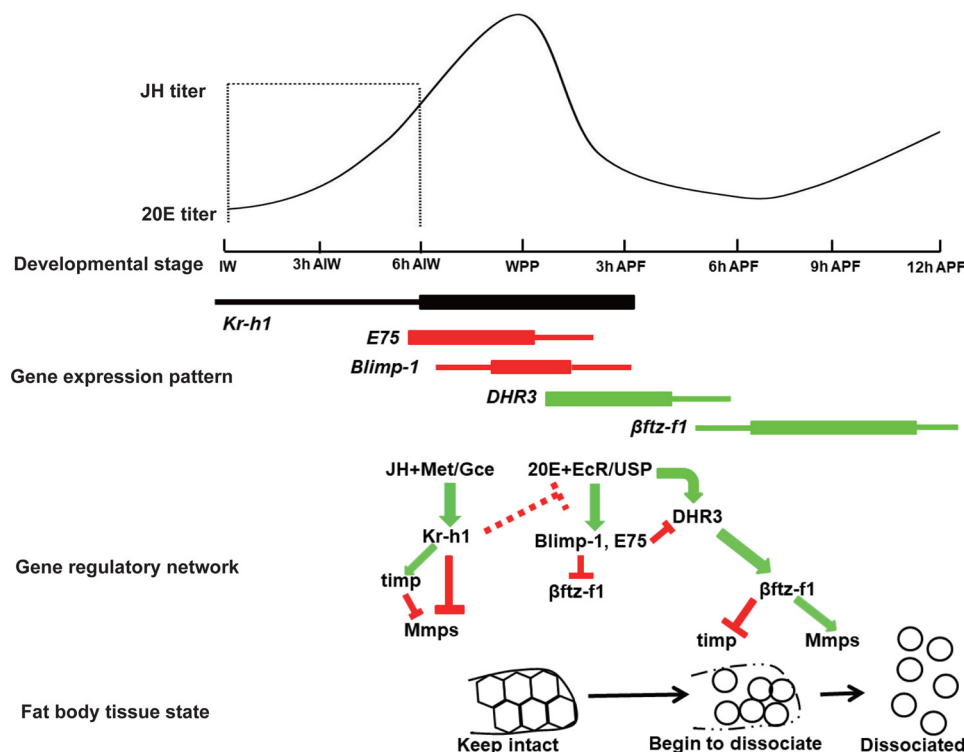
Figure 7. Model showing developmental timing of Mmp–induced fat body cell dissociation is coordinately and precisely controlled by JH and 20E in *Drosophila*. During larval–prepupal transition, the anti-metamorphic factor Kr-h1 transduces JH signaling to directly inhibit *Mmp* expression and to activate *timp* expression and thus suppresses Mmp–induced fat body cell dissociation. When JH titer declines, the prepupal peak of 20E suppresses Mmp–induced fat body cell dissociation through the 20E primary-response genes, *E75* and *Blimp-1*, which inhibit *βftz-F1* expression indirectly or directly. Until 20E titer declines, *βftz-F1* expression is induced by the 20E early–late response gene *DHR3*; then *βftz-F1* directly activates *Mmp* expression and inhibits *timp* expression and causes Mmp–induced fat body cell dissociation occurring from 6 h APF to 12 h APF. The JH and 20E titers are depicted according to Dubrovsky 2005 (30).

the detailed molecular mechanisms by which JH and 20E precisely control the developmental timing of Mmp–induced fat body cell dissociation at both mRNA and enzymatic levels in *Drosophila*, and we provided a working model of hormonal control of tissue remodeling in animals (Fig. 7). In summary, at first, Kr-h1 transduces JH signaling to inhibit Mmp–induced fat body cell dissociation during larval–prepupal transition. Then when JH titer declines, the prepupal peak of 20E suppresses Mmp–induced fat body cell dissociation through *E75* and *Blimp-1*, which inhibit *βftz-F1* expression. Finally, until 20E titer declines, DHR3 induces *βftz-F1* expression, and *βftz-F1* covers the 20E-triggered transcriptional cascade to activate Mmp–induced fat body cell dissociation within 6 h before pupation. This study provides an excellent sample for better understanding the hormonal regulation of insect metamorphosis.

Experimental procedures

Flies and genetics

All fly strains were grown at 25 °C on standard cornmeal/molasses/agar medium. Synchronization was performed at IW or WPP as previously described (35). *UAS-Kr-h1-V5* and *UAS-Blimp-1* transgenic flies were produced via P-element–mediated germ-line transformation (29). *w1118*, *Aug21-GAL4*, *Lsp2-GAL4*, *UAS-grim*, *UAS-EcRDN*, *Met27 gce2.5k*, and *Kr-h1k04411* were reported previously (2, 19, 21, 23, 24, 29, 35). Notably, *Lsp2-Gal4* is specifically expressed in the fat body during larval–pupal metamorphosis (15). *UAS-ftz-f1-RNAi* (v2959), *UAS-Blimp-1-dsRNA* (v108374), and *UAS-timp-dsRNA* (v109427) flies were obtained from the Vienna *Drosophila* RNAi Center. The *UAS-E75A, UAS-E75-dsRNA, UAS-DHR3*, and *UAS-DHR3-dsRNA* flies were generously provided by Dr. Jiong Chen (36). The *UAS-βftz-F1* fly was presented by Dr. Rosa Barrio (37). The *timp* mutant flies was presented by Dr. Buchner (38). All flies were crossed with the wild-type *w1118* eight times to minimize the effects of the genetic background. Other flies used in this paper were generated by recombination.

Quantitative measurements of fat body cell dissociation

The degree of fat body cell dissociation was measured as previously described in detail (2). Fat body tissues at 6 h APF from different genotypes were used to evaluate whether premature fat body dissociation happened. Fat body tissues at 12 h APF from different genotypes were used to evaluate whether delayed fat body cell dissociation happened. In this assay, 10 animals

Figure 6. JH signaling promotes *timp* expression, and *βftz-F1* inhibits *timp* expression. *A, timp* expression in the fat body of the JH signaling-deficient animals at 6 h APF (*left panel*) and in the fat body of *Kr-h1*–overexpressing animals at 12 h APF (*right panel*). *B, timp* expression in the fat body of *EcRDN*-overexpressing and *βftz-F1* RNAi animals at 12 h APF (*left panel*) and in the fat body of *βftz-F1*-overexpressing animals at 6 h APF (*right panel*). *C,* Mmps enzymatic activity in the fat body of JH signaling-deficient animals and *βftz-F1*-overexpressing animals at 6 h APF (*upper panel*) as well as in the fat body of *EcRDN*-overexpressing, *βftz-F1* RNAi, and *Kr-h1*–overexpressing animals (*lower panel*).

were used for each independent genotype, and three independent replications were carried out.

Cell culture and transient transfection

Drosophila Kc cells were cultured in Schneider's *Drosophila* medium (Sigma–Aldrich) supplemented with 5% fetal bovine serum (HyClone). The pActin-GAL4 plasmid was constructed in our laboratory. *Kr-h1* and *Blimp-1* cDNA was cloned into the pUAST vector to obtain pUAST-Kr-h1-V5 and pUAST-Blimp-1, respectively. The pUAST-3×flag-βftz-F1 (37) construct was generously provided by Dr. Rosa Barrio. Transient transfection in Kc cells was performed as previously described in detail (2, 24).

qPCR and Western blotting

qPCR and Western blotting were performed as described previously (2). Rp49 was chosen as the reference gene for qPCR analysis. Our previous studies showed that Western blotting detected four major bands (46, 52, 64, and 74 kDa) and two major bands (90 and 120 kDa) for Mmp1 and Mmp2, respectively, in the *Drosophila* fat body (2).

Dual luciferase assay

To identify KBS, a 3-kb region of the *Mmp1* promoter upstream of the transcription start site was cloned into the SmaI and BglII sites of the pGL3-Basic vector. Likewise, to identify βftz–FBS, a 3-kb region of the *Mmp2* promoter upstream of the transcription start site was cloned into the SmaI and BglII sites of the pGL3-Basic vector. Deletions and mutations in *Mmp1* promoter regions were also constructed in the pGL3-Basic vector. The −1473 to −1308 fragment, the KBS CTCAATAACCTAT-GCCACAT and 4×CTCAATAACCTATGCCACAT sequence were cloned into the SmaI and BglII sites of the pGL3-promoter vector. After transient transfection into Kc cells with the pGL3 reporter vector and the pRL reference vector, dual luciferase assays were performed as previously described (13, 24, 39).

Electrophoretic mobility shift assay

Kr-h1 cDNA was inserted into a pET28a vector with a 6×His tag at the N terminus. Then the plasmid was transformed into the *Escherichia coli* Rosetta strain. The transformed bacterial cells were grown in LB medium supplemented with kanamycin (0.1 mg/ml) at 37 °C and induced by 0.25 mM isopropyl β-D-thiogalactopyranoside for 12 h at 16 °C. The cells were harvested and resuspended in buffer A (20 M Tris-HCl (H8.0) and 100 M NaCl) supplemented with 1 mM PMSF. Cells were lysed using a high-pressure cell disruptor at 18,000 p.s.i., and the lysate was centrifuged at 16,000 × g for 45 min. The supernatant was loaded onto a Ni^{2+}-nitrilotriacetic acid affinity column (Qiagen) and washed with buffer A plus 20 mM imidazole. Proteins were eluted with buffer A plus 250 mM imidazole and purified further by gel filtration using a Superdex 200 column (GE Healthcare) in buffer A. Peak fractions were collected and concentrated for subsequent studies (40). βftz-F1 cDNA was cloned into the pGEX-4T-1 vector, and GST-βftz-F1 proteins were expressed and purified in Rosetta cells using standard methods as previously described (32). EMSA was performed according to our previous publication (41).

Chromatin immunoprecipitation

At 48 h after transfection, 3× FLAG-βftz-F1-overexpressing Kc cells were fixed and subjected to ChIP using the Pierce™ agarose ChIP kit (26156; Thermo) and the FLAG mouse monoclonal antibody (F3156; Sigma–Aldrich). Mock immunoprecipitations with preimmune serum were performed as negative controls. The precipitated DNA and input were analyzed by qPCR to detect binding ability (13, 39).

Statistics

Experimental data were analyzed with analysis of variance and Student's *t* test. Analysis of variance is shown as the bars labeled with different lowercase letters as significantly different ($p < 0.05$; *t* test: *, $p < 0.05$; **, $p < 0.01$; ***, $p < 0.001$). Throughout the paper, values are represented as the means ± standard deviation of 3–10 independent experiments.

References

1. Nelliot, A., Bond, N., and Hoshizaki, D. K. (2006) Fat-body remodeling in *Drosophila melanogaster*. *Genesis* **44,** 396–400
2. Jia, Q., Liu, Y., Liu, H., and Li, S. (2014) Mmp1 and Mmp2 cooperatively induce *Drosophila* fat body cell dissociation with distinct roles. *Sci. Rep.* **4,** 7535
3. Bond, N. D., Nelliot, A., Bernardo, M. K., Ayerh, M. A., Gorski, K. A., Hoshizaki, D. K., and Woodard, C. T. (2011) βftz-F1 and matrix metalloproteinase 2 are required for fat-body remodeling in *Drosophila*. *Dev. Biol.* **360,** 286–296
4. Gaffney, J., Solomonov, I., Zehorai, E., and Sagi, I. (2015) Multilevel regulation of matrix metalloproteinases in tissue homeostasis indicates their molecular specificity *in vivo*. *Matrix Biol.* **44,** 191–199
5. Page-McCaw, A., Serano, J., Santé, J. M., and Rubin, G. M. (2003) *Drosophila* matrix metalloproteinases are required for tissue remodeling, but not embryonic development. *Dev. Cell* **4,** 95–106
6. Page-McCaw, A., Ewald, A. J., and Werb, Z. (2007) Matrix metalloproteinases and the regulation of tissue remodelling. *Nat. Rev. Mol. Cell Biol.* **8,** 221–233
7. Riddiford, L. M., Cherbas, P., and Truman, J. W. (2000) Ecdysone receptors and their biological actions. *Vitam. Horm.* **60,** 1–73
8. Yamanaka, N., Rewitz, K. F., and O'Connor, M. B. (2013) Ecdysone control of developmental transitions: lessons from *Drosophila* research. *Annu. Rev. Entomol.* **58,** 497–516
9. Lam, G. T., Jiang, C., and Thummel, C. S. (1997) Coordination of larval and prepupal gene expression by the DHR3 orphan receptor during *Drosophila* metamorphosis. *Development* **124,** 1757–1769
10. Lam, G., Hall, B. L., Bender, M., and Thummel, C. S. (1999) DHR3 is required for the prepupal–pupal transition and differentiation of adult structures during *Drosophila* metamorphosis. *Dev. Biol.* **212,** 204–216
11. White, K. P., Hurban, P., Watanabe, T., and Hogness, D. S. (1997) Coordination of *Drosophila* metamorphosis by two ecdysone-induced nuclear receptors. *Science* **276,** 114–117
12. Parvy, J. P., Wang, P., Garrido, D., Maria, A., Blais, C., Poidevin, M., and Montagne, J. (2014) Forward and feedback regulation of cyclic steroid production in *Drosophila melanogaster*. *Development* **141,** 3955–3965
13. Li, K., Tian, L., Guo, Z., Guo, S., Zhang, J., Gu, S.-H., Palli, S. R., Cao, Y., and Li, S. (2016) 20-hydroxyecdysone (20E) primary response gene E75 isoforms mediate steroidogenesis autoregulation and regulate developmental timing in *Bombyx*. *J. Biol. Chem.* **291,** 18163–18175

14. Akagi, K., Sarhan, M., Sultan, A. R., Nishida, H., Koie, A., Nakayama, T., and Ueda, H. (2016) A biological timer in the fat body comprising Blimp-1, βftz-F1 and Shade regulates pupation timing in *Drosophila melanogaster*. *Development* **143**, 2410–2416

15. Cherbas, L., Hu, X., Zhimulev, I., Belyaeva, E., and Cherbas, P. (2003) EcR isoforms in *Drosophila*: testing tissue-specific requirements by targeted blockage and rescue. *Development* **130**, 271–284

16. Jindra, M., Palli, S. R., and Riddiford, L. M. (2013) The juvenile hormone signaling pathway in insect development. *Annu. Rev. Entomol.* **58**, 181–204

17. Jindra, M., Bellés, X., and Shinoda, T. (2015) Molecular basis of juvenile hormone signaling. *Curr. Opin. Insect Sci.* **11**, 39–46

18. Godlewski, J., Wang, S., and Wilson, T. G. (2006) Interaction of bHLH-PAS proteins involved in juvenile hormone reception in *Drosophila*. *Biochem. Biophys. Res. Commun.* **342**, 1305–1311

19. Abdou, M. A., He, Q., Wen, D., Zyaan, O., Wang, J., Xu, J., Baumann, A. A., Joseph, J., Wilson, T. G., Li, S., and Wang, J. (2011) *Drosophila* Met and Gce are partially redundant in transducing juvenile hormone action. *Insect Biochem. Mol. Biol.* **41**, 938–945

20. Jindra, M., Uhlirova, M., Charles, J. P., Smykal, V., and Hill, R. J. (2015) Genetic evidence for function of the bHLH-PAS protein Gce/Met as a juvenile hormone receptor. *PLoS Genet.* **11**, e1005394

21. Wen, D., Rivera-Perez, C., Abdou, M., Jia, Q., He, Q., Liu, X., Zyaan, O., Xu, J., Bendena, W. G., Tobe, S. S., Noriega, F. G., Palli, S. R., Wang, J., and Li, S. (2015) Methyl farnesoate plays a dual role in regulating *Drosophila* metamorphosis. *PLoS Genet.* **11**, e1005038

22. Minakuchi, C., Zhou, X., and Riddiford, L. M. (2008) *Kruppel homolog* 1 (*Kr-h1*) mediates juvenile hormone action during metamorphosis of *Drosophila melanogaster*. *Mech. Dev.* **125**, 91–105

23. Huang, J., Tian, L., Peng, C., Abdou, M., Wen, D., Wang, Y., Li, S., and Wang, J. (2011) DPP-mediated TGF-β signaling regulates juvenile hormone biosynthesis by upregulating expression of JH acid methyltransferase. *Development* **138**, 2283–2291

24. He, Q., Wen, D., Jia, Q., Cui, C., Wang, J., Palli, S. R., and Li, S. (2014) Heat shock protein 83 (Hsp83) facilitates methoprene-tolerant (Met) nuclear import to modulate juvenile hormone signaling. *J. Biol. Chem.* **289**, 27874–27885

25. Belles, X., and Santos, C. G. (2014) The MEKRE93 (methoprene tolerant-Kruppel homolog 1-E93) pathway in the regulation of insect metamorphosis, and the homology of the pupal stage. *Insect Biochem. Mol. Biol.* **52**, 60–68

26. Ureña, E., Chafino, S., Manjón, C., Franch-Marro, X., and Martín, D. (2016) The occurrence of the holometabolous pupal stage requires the interaction between E93, Krüppel-homolog 1 and Broad-complex. *PLoS Genet.* **12**, e1006020

27. Kayukawa, T., Nagamine, K., Ito, Y., Nishita, Y., Ishikawa, Y., and Shinoda, T. (2016) Krüppel homolog 1 inhibits insect metamorphosis via direct transcriptional repression of *Broad-complex*, a pupal specifier gene. *J. Biol. Chem.* **291**, 1751–1762

28. Kayukawa, T., Jouraku, A., Ito, Y., and Shinoda, T. (2017) Molecular mechanism underlying juvenile hormone-mediated repression of precocious larval-adult metamorphosis. *Proc. Natl. Acad. Sci. U.S.A.* **114**, 1057–1062

29. Liu, Y., Sheng, Z., Liu, H., Wen, D., He, Q., Wang, S., Shao, W., Jiang, R.-J., An, S., Sun, Y., Bendena, W. G., Wang, J., Gilbert, L. I., Wilson, T. G., Song, Q., *et al.* (2009) Juvenile hormone counteracts the bHLH-PAS transcription factors MET and GCE to prevent caspase-dependent programmed cell death in *Drosophila*. *Development* **136**, 2015–2025

30. Dubrovsky, E. B. (2005) Hormonal cross talk in insect development. *Trends Endocrinol. Metab.* **16**, 6–11

31. Pecasse, F., Beck, Y., Ruiz, C., and Richards, G. (2000) Kruppel-homolog, a stage-specific modulator of the prepupal ecdysone response, is essential for *Drosophila* metamorphosis. *Dev. Biol.* **221**, 53–67

32. Bowler, T., Kosman, D., Licht, J. D., and Pick, L. (2006) Computational identification of Ftz/Ftz-f1 downstream target genes. *Dev. Biol.* **299**, 78–90

33. Pearson, J. R., Zurita, F., Tomás-Gallardo, L., Díaz-Torres, A., Díaz de la Loza, M., Franze, K., Martín-Bermudo, M., and González-Reyes, A. (2016) ECM-regulator *timp* is required for stem cell niche organization and cyst production in the *Drosophila* ovary. *PLoS Genet.* **12**, e1005763

34. Clark, I. M., Swingler, T. E., Sampieri, C. L., and Edwards, D. R. (2008) The regulation of matrix metalloproteinases and their inhibitors. *Int. J. Biochem. Cell Biol.* **40**, 1362–1378

35. Liu, H., Jia, Q., Tettamanti, G., and Li, S. (2013) Balancing crosstalk between 20-hydroxyecdysone-induced autophagy and caspase activity in the fat body during *Drosophila* larval–prepupal transition. *Insect Biochem. Mol. Biol.* **43**, 1068–1078

36. Luo, J., Zuo, J., Wu, J., Wan, P., Kang, D., Xiang, C., Zhu, H., and Chen, J. (2015) *In vivo* RNAi screen identifies candidate signaling genes required for collective cell migration in *Drosophila* ovary. *Sci. China Life Sci.* **58**, 379–389

37. Talamillo, A., Herboso, L., Pirone, L., Pérez, C., González, M., Sánchez, J., Mayor, U., Lopitz-Otsoa, F., Rodriguez, M. S., Sutherland, J. D., and Barrio, R. (2013) Scavenger receptors mediate the role of SUMO and Ftz-f1 in *Drosophila* steroidogenesis. *PLoS Genet.* **9**, e1003473

38. Godenschwege, T. A., Pohar, N., Buchner, S., and Buchner, E. (2000) Inflated wings, tissue autolysis and early death in *tissue inhibitor of metalloproteinases* mutants of *Drosophila*. *Eur. J. Cell Biol.* **79**, 495–501

39. Liu, X., Dai, F., Guo, E., Li, K., Ma, L., Tian, L., Cao, Y., Zhang, G., Palli, S. R., and Li, S. (2015) 20-hydroxyecdysone (20E) primary-response gene E93 modulates 20E signaling to promote *Bombyx* larval–pupal metamorphosis. *J. Biol. Chem.* **290**, 27370–27383

40. Qi, X., Lin, W., Ma, M., Wang, C., He, Y., He, N., Gao, J., Zhou, H., Xiao, Y., Wang, Y., and Zhang, P. (2016) Structural basis of rifampin inactivation by rifampin phosphotransferase. *Proc. Natl. Acad. Sci. U.S.A.* 113, 3803–3808

41. Tian, L., Ma, L., Guo, E., Deng, X., Ma, S., Xia, Q., Cao, Y., and Li, S. (2013) 20-hydroxyecdysone upregulates Atg genes to induce autophagy in the *Bombyx* fat body. *Autophagy* **9**, 1172–1187